Omondi, RO, Ojwach, SO, Jaganyi, D and Fatokun, AA

(Pyrazolyl)pyridine ruthenium(III) complexes: Synthesis, kinetics of substitution reactions with thiourea and biological studies

(Pyrazolyl)pyridine ruthenium(III) complexes: Synthesis, kinetics of substitution reactions with thiourea and biological studies

Reinner O. Omondi, [1] Stephen O. Ojwach,* [1] Deogratius Jaganyi, [1] Amos A. Fatokun [2]

[1]School of Chemistry and Physics, University of KwaZulu-Natal, Private Bag X01, Scottsville, Pietermaritzburg, 3209, South Africa

[2]School of Pharmacy and Biomolecular Sciences, Faculty of Science, Liverpool John Moores University, Liverpool L3 3AF, England, UK

Abstract

Reactions of 2-bromo-6-(3,5-dimethyl-1H-pyrazol-1-yl)pyridine (**L1**), 2,6-di (1H-pyrazol-1-yl) pyridine (**L2**) and 2,6-bis(3,5-dimethyl-1H-pyrazol-1-yl)pyridine (**L3**) with $RuCl_3 \cdot 3H_2O$ led to the formation of their respective metal complexes [$RuCl_3$(**L1**)] (**1**), [$RuCl_3$(**L2**)] (**2**) and [$RuCl_3$(**L3**)] (**3**). Solid state structure of complex **3** established the formation of a six-coordinate mononuclear compound in which **L3** is tridentately bound. The order of reactivity of the studied complexes with thiourea (**TU**) nucleophile is in the form **1** > **2** > **3**, in line with density functional theory (DFT) studies. The complexes displayed minimal cytotoxic activity against the HeLa cell line, consistent with molecular docking experiments which showed weaker DNA binding affinities.

Keywords: ruthenium complexes; ligand substitution; cytotoxicity, anti-cancer activities; DFT; molecular docking

*Corresponding author: Tel.: +27 (33) 260 5239; Fax: +27 (33) 260 5009

E-mail: ojwach@ukzn.ac.za (S. O. Ojwach)

Cancer is the second leading cause of death globally, only surpassed by cardiovascular diseases, with nearly 1 in 6 deaths due to cancer [1]. Following the discovery of the platinum-based drug *cisplatin* for treating cancer, a wide spectrum of platinum(II)-based complexes have been developed and are commercially available, e.g., *carboplatin* [2]. However, there are currently limitations to the clinical use of *cisplatin* and its analogues, e.g., dose-limiting toxicity and resistance [3]. Thus, there has been a surge in the development of alternative drugs without the demerits of platinum-based analogues. Notable examples include the ruthenium(II) compounds which have shown some promising results [4]. However, a key challenge in the development of metal-based drugs lies in understanding the drug-host interactions, in addition to the intrinsic properties of the complexes. Therefore, to have a better understanding of the mechanisms and mode of action of metallo-drugs, a combination of experimental and theoretical platforms is critical and is currently being explored. These include studying the kinetics of substitution reactions [5] with biologically relevant molecules, molecular docking [6] and DNA binding studies [7].

As an illustration, Bratsos *et al.* established that anticancer activities of ruthenium(II) half sandwich complexes are directly related to the rate of hydrolysis of the complexes [8]. In a more recent study, the anti-cancer activities of two ruthenium(II) complexes, [Ru(Cl-tpy)(en)Cl][Cl] and Ru(Cl-tpy)(dach)Cl][Cl] reveal that the lower rate of substitution of the coordinated chloride ligand with biologically relevant L-His in comparison to 5′-GMP is responsible for their anti-tumor activity due limited cytoplasmic deactivation [9]. An example where DNA binding and molecular docking has been used to interrogate the cytotoxicity of metal compounds is well presented in the recent report of Hong *et al.* [10] using enantiomeric ruthenium(II) complexes. A positive correlation between the binding affinities of the compounds to the DNA and their anti-cancer activities was observed. In this communication, we report the application of a combination of kinetics of ligand substitution reactions,

molecular docking and theoretical studies to investigate the anti-cancer activities of (pyrazolyl)pyridine ruthenium(III) compounds.

The compounds, 2-bromo-6-(3,5-dimethyl-1H-pyrazol-1-yl)pyridine (**L1**), 2,6-di (1H-pyrazol-1-yl) pyridine (**L2**) and 2,6-bis(3,5-dimethyl-1H-pyrazol-1-yl)pyridine (**L3**) ligands were synthesised following literature methods [11]. Reactions of **L1**-**L3** with $RuCl_3 \cdot 3H_2O$ resulted in the formation of the corresponding ruthenium(III) metal complexes **1**-**3** in good yields (Scheme 1). Mass spectrometry, elemental analyses and single crystal X-ray analyses was used to characterize the complexes. For example, the ESI-MS mass spectrum of complex **3** (Figure S1) showed a base peak at 439.01 amu, corresponding to the $[Ru(\mathbf{L3})Cl_2]^+$ fragment. The elemental analyses data of complexes **1**–**3** were in good agreement with one metal centre and one ligand motif as proposed in Scheme 1. While penta-coordinated Ru(III) complexes are rare, both the elemental analyses and MS (m/z = 424.85: M+ - Cl) data collected for complex **1** agree with the proposed structure. However, it is possible that the crystal structure of **1** may contain a solvent molecule in the sixth coordination sphere as we previously reported for similar Ru(III) complexes [12].

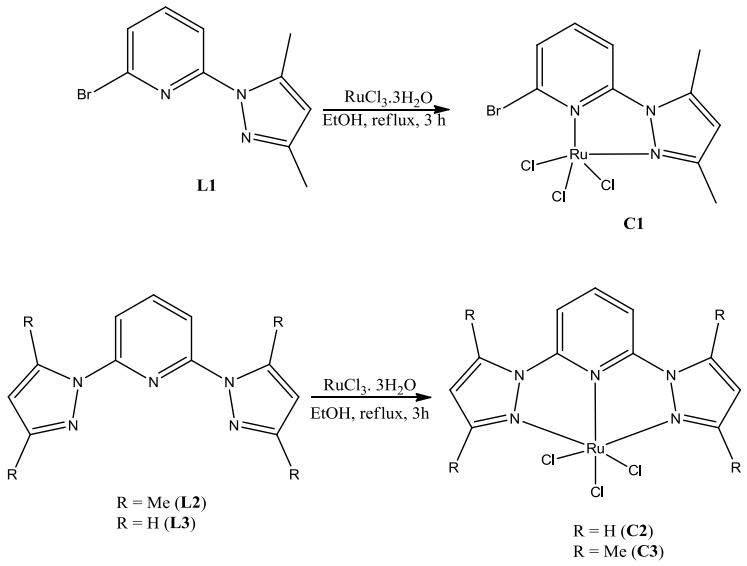

Scheme 1: Syntheses of (pyrazolyl)pyridine ruthenium(III) complexes **1**-**3**.

The molecular structure of complex **3** is shown in Figure 1, while Table S1 contains crystallographic data and structure refinement parameters. The coordination around the metal atom consists of one tridentate ligand **L3** and three chloride ligands to give a six-coordination environment. The bond angles for instance N(5)-Ru(1)-Cl(1) of 91.82° deviate from 90°, consistent with a distorted octahedral geometry. The shorter bond distances for Ru-Cl(1) and Ru-Cl(2) of 2.3540(5) and 2.3303(5) Å respectively with respect to the bond length for Ru-Cl(3) of 2.4122(5) Å is attributed to the different *trans* influence of the pyridine nitrogen atom in comparison to the chloride atom. The pyrazole and pyridine rings are in the same plane, with dihedral angles of 79.49° and 79.36° respectively, in good agreement with those reported for similar ruthenium(III) complexes [13]. The average Ru-N_{pz}, Ru-N_{py} and Ru-Cl bond lengths of 2.0639(15) Å, 1.9698(14) Å and 2.3655(5) Å in **3** compare well with the average bond distances of 2.086(2) Å, 1.988(2) Å and 2.3531(6) Å, respectively, for a recently reported 2,6-bis-(3′,5′-diphenylpyrazolyl)pyridine ruthenium(III) complex [14].

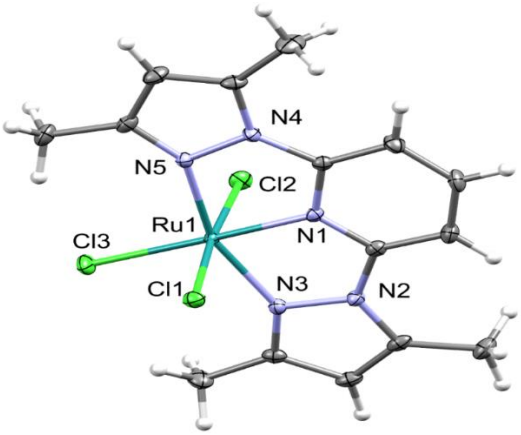

Figure 1: Molecular structure diagram of **3**. Selected bond lengths (Å) and angles (°): Ru(1)-N(1), 1.9698(14); Ru(1)-N(3), 2.0518(15); Ru(1)-N(5), 2.0760(15); Ru(1)-Cl(2), 2.3303(5); Ru(1)-Cl(1), 2.3540(5), Ru(1)-Cl(3), 2.4122(5); N(1)-Ru(1)-N(3), 79.49(6); N(3)-Ru(1)-N(5), 158.85(6); N(3)-Ru(1)-Cl2(2), 88.08(5); N(5)-Ru(1)-Cl(2), 90.61(4); N(5)-Ru(1)-Cl(1), 91.82(4); Cl(2)-Ru(1)-Cl(1), 174.906(16), N(3)-Ru(1)-Cl(3), 100.65(4); Cl(1)-Ru(1)-Cl(3), 92.095(17).

The kinetics of ligand substitution reactions of complexes **1-3** with the biologically relevant thiourea (TU) was investigated. All the substitution reactions fitted into a single exponential decay, an indication that the three chloro atoms were substituted by thiourea simultaneously (Figure S2). Plots of k_{obs} against the concentration of the incoming nucleophile gave straight line with zero intercept which means that the substitution reactions can be represented as shown in Figure 2, Scheme 2 and Equation 1. The values of the second order rate constant, k_2, were obtained from the slopes of these plots (Figures S3) at 25 °C and are summarised in Table 2. Additional kinetics plots and data are given in supplementary Figures S3-S9 and Tables S2-S5.

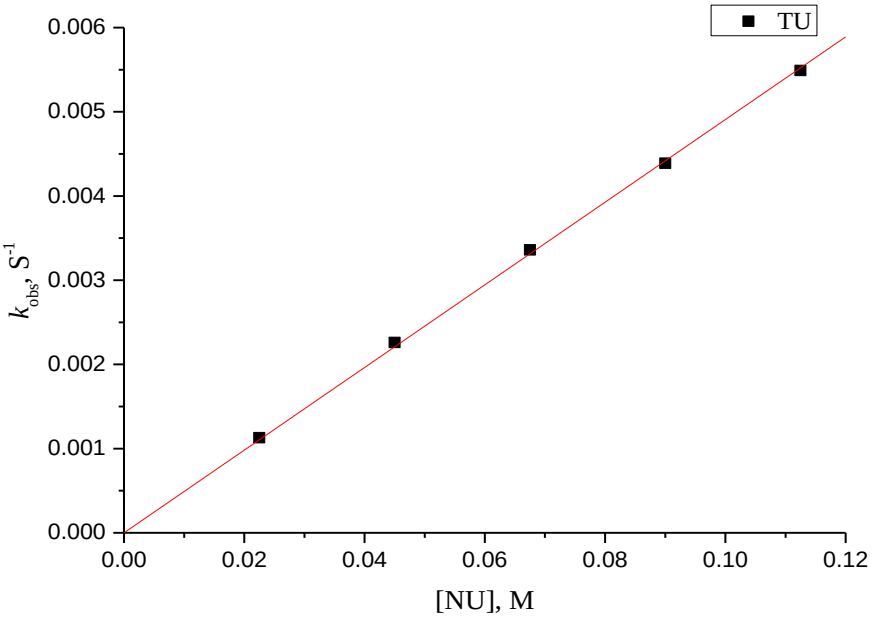

Figure 2: Concentration dependence of k_{obs} for the substitution of chlorides from **1** (5.0×10^{-4} M) by TU (0.225 M) in methanol solution, I = 0.1 M (adjusted with $NaClO_4$/LiCl) at 298 K.

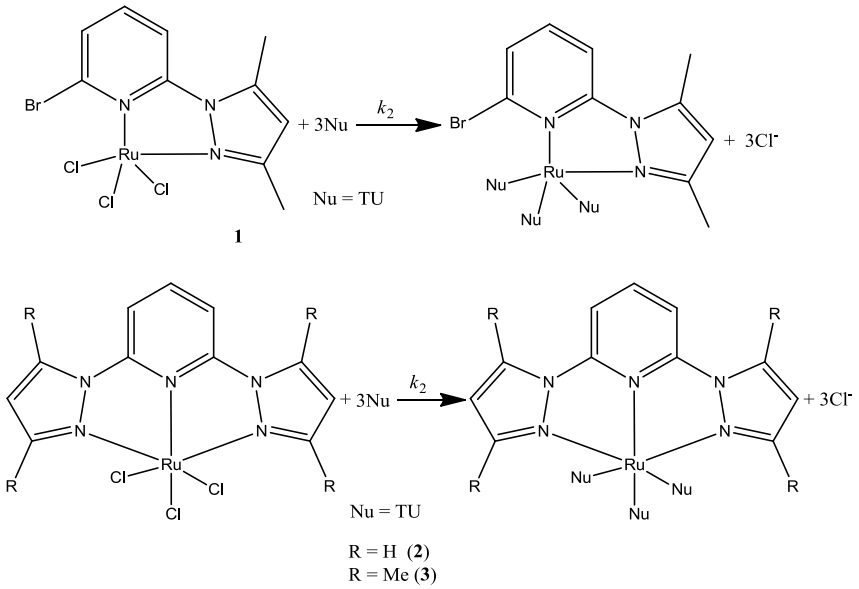

Scheme 2: Proposed substitution mechanism for the mononuclear (pyrazolyl)pyridine ruthenium(III) complexes **1-3** with thiourea nucleophile.

$$k_{obs} = k_2 [Nu] \quad (1)$$

Table 2: Summary of the rate constants and activation parameters for the substitution of chloride ligand by TU nucleophile in complexes **1-3**.[a]

Complex	**Nu**	**k_2/M^{-1}s^{-1}×10^{-2}**	**Δ*H*/kJmol^{-1}**	**Δ*S*/Jmol^{-1}K^{-1}**
1	TU	5.00 ± 0.03	56 ± 1	-105 ± 3
2	TU	2.25 ± 0.01	63 ± 1	-60 ± 3
3	TU	0.24 ± 0.00	71 ± 1	-38 ± 3

[a]Solvent: methanol, I = 0.1 M (adjusted with $NaClO_4$/LiCl) at 298 K

The temperature dependence studies were carried out using a temperature range of 25-45 °C in 5 °C intervals. The thermodynamic parameters, activation enthalpies, $\Delta H^{\neq}$, and the activation entropies, $\Delta S^{\neq}$, were calculated from the slopes and the intercepts of the Eyring plots (Figures 3, S4-S5 and Tables S5-S7) and are presented in Table 2. Computational modelling of the ruthenium(III) complexes was performed in order to provide insight to kinetics data. The geometry optimised structures and the frontier orbitals are given in Table S8 while a summary

of the respective HOMO-LUMO energies, chemical hardness, chemical potential, global electrophilicity index, NBO atomic charges and dipole moments are shown in Table 3.

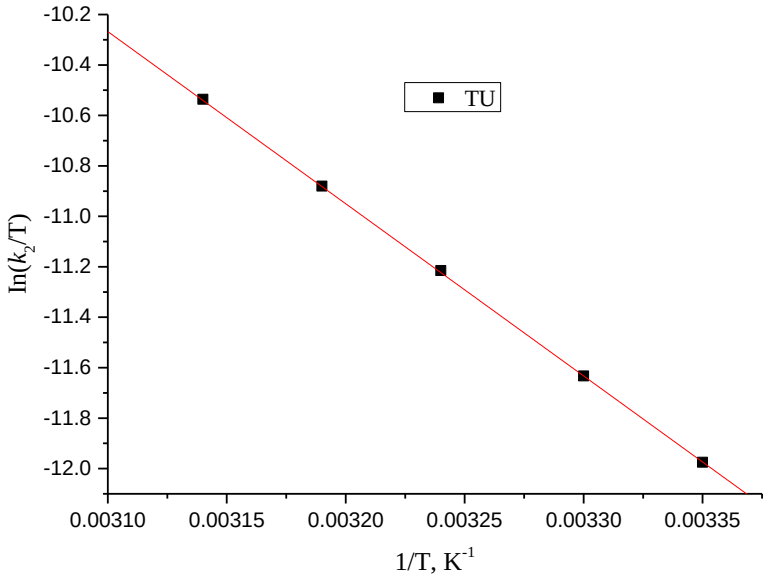

Figure 3: Eyring plot obtained for the substitution of chloride from **1** by thiourea nucleophiles in methanolic solution, I = 0.1 M (0.01 M LiCl, 0.09 M $NaClO_4$) at various temperatures in the range 25 - 45 °C.

Table 3: Summary of the data obtained from the DFT calculations for complexes **1-3**

Parameter	**1**	**2**	**3**
LUMO /eV	-3.27	-2.66	-2.50
HOMO /eV	-6.90	-6.60	-6.49
ΔE /eV	3.64	3.94	4.09
η/eV	1.82	1.97	2.05
μ/eV	-5.08	-4.63	-4.44
ω/eV	7.11	5.45	4.82
Ru NBO charges	0.35	0.35	0.34
Dipole moment (D)	20.52	19.52	17.49

η = chemical hardness, μ = chemical potential and ω = global electrophilicity index. NBO = natural bond orbital.

Comparing the rates of displacement of the coordinated chlorides by the thiourea nucleophile, the order of decreasing reactivity was found to be **1** > **2** > **3**. The difference in

reactivity can be concluded to be due to electronic effects. This is supported by the DFT calculations which shows that the electrophilicity of the complexes are in line with the trend of the rates of the substitution reactions. To try and understand the observed reactivity trend, it is important to reflect on the properties of the spectator ligand. The pyridine ring readily accepts π-back bonding from the metal, while pyrazole rings are π-electron rich because of the extra pyrazolyl-N which make them better σ-donors [15-16]. This means that the pyrazole fragment has poor π-acceptor ability and good σ-donor ability. This property results in accumulation of electron density around the metal atom with a net reduction in the substitution of the chloro atom. In the present study, complex **1** is more reactive than **2** and **3** due to its higher electrophilicity compared to complexes **2** and **3**, which contain an extra pyrazolyl motif.

Secondly, the pyridine ring has an electron withdrawing bromide group [17] and thereby, enhancing the π-back bonding ability of the ring. Comparing complexes **2** and **3**, the controlling factor is the presence of the pyrazolyl methyl substituents in **3**. This enhances the σ-donor ability of the pyrazole ring while reducing its π-acceptor properties and thus makes the metal centre to be the least electropositive as supported by the DFT calculations and elecetrophilicity values (ω). In addition, the DFT calculations also support the role of the π-back donation [18] through the values of dipole moments which shows a trend of 20.52 > 19.52 > 17.49 for **1**, **2** and **3** respectively. The overall substitution mechanism is associative in nature as supported by the large negative $\Delta S^{\neq}$ values and relatively small $\Delta H^{\neq}$ values. This means that the transition state is highly ordered accompanied with an easy bond formation [19].

The *in vitro* cytotoxicity of the investigated compounds against cultured HeLa cells was determined by assessing cell viability using the MTT assay, with the anti-cancer drug doxorubicin used as a positive control. Viability was assessed after incubating the cells with the compounds for 48 h. The effects on cell viability of the anti-cancer drug, doxorubicin, used as a positive control, as well as the effects of the ligands and their corresponding complexes

are shown in Figure 4, while representative images showing changes to cell morphology induced by the various concentrations of the compounds are given in Figure S6. Doxorubicin decreased cell viability in a concentration-dependent manner (*P<0.05, **P<0.01, ***P<0.001), with an average IC_{50} of 0.8±0.2 µM (n=3). These deleterious effects of doxorubicin on cell viability are correlated, through brightfield microscopic examination, with progressive loss of cells and the rounding up of the remaining cells (Figure S6). The results show that the (pyrazolyl)pyridine ligands generally displayed relatively higher cytotoxic activities than their respective ruthenium(III) metal complexes, as indicated by changes to viability (Figure 4) and morphology (Figure S6). For instance, **L2**, reduced viability concentration-dependently (IC_{50} of **L2** = 83 µM) and, was significantly more cytotoxic than complex **2** (IC_{50} > 200 µM i.e no significant effect at concentrations tested). The difference could be due to the limited solubility of the complexes in DMSO [20], as we could not test the complexes beyond 100 µM while it was possible to test concentrations of the ligands up to 400 µM. The minimal cytotoxicity of both the ligands and their complexes **1**-**3** as revealed by their relatively high IC_{50} values may be due to minimal aromaticity of the (pyrazolyl)pyridine ligands, which ultimately limits the interaction of the compounds with the DNA [20]. While there is no well documented relationship between ligand substitution reactions and anti-cancer activity, the favourable reactions of complexes **1**-**3** with TU may lead to cytoplasmic deactivation of the compounds before reaching the targeted DNA molecule [6]. Another factor that may account for the low activity of the compounds could be the resistant nature of the HeLa cell line compared to other cancer cell types [21].

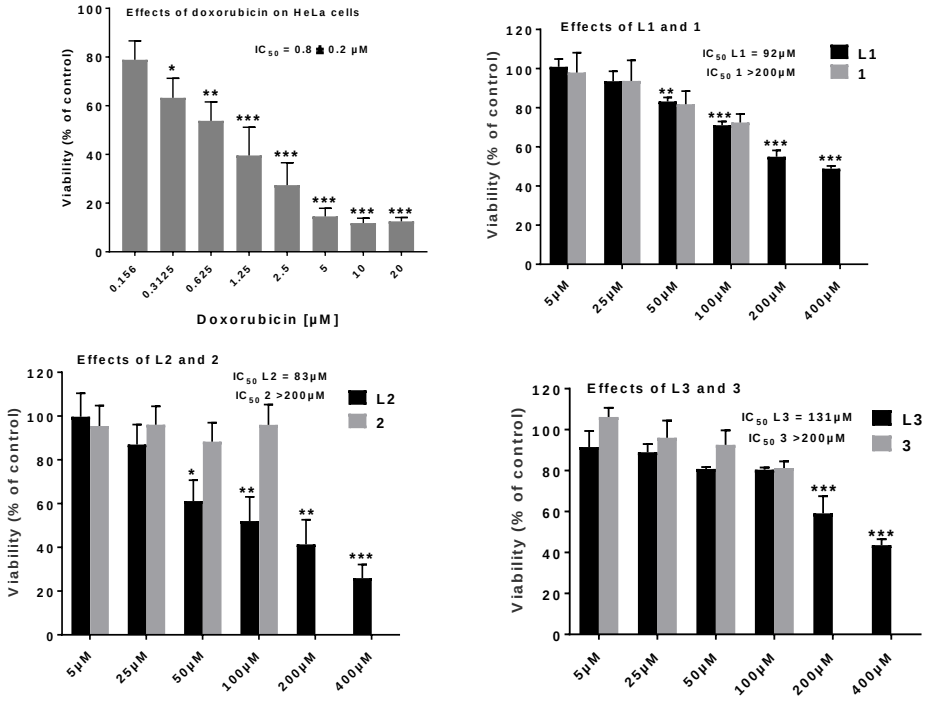

Figure 4: Effects on the viability of HeLa cells of anti-cancer drug, doxorubicin (used as positive control), ligands **L1**-**L3**, and complexes **1**-**3**. IC_{50} values are as indicated on the graphs. *P<0.05, **P<0.01 and ***P<0.001 compared to the negative control. Values shown are Mean ± SEM of 3-4 independent experiments.

To examine the binding affinities and sites of complexes **1**-**3** to DNA, molecular docking studies were carried out on complexes **1**-**3** with B-DNA (PDB ID: 1BNA). Docked images and relative binding energies of the investigated complexes are shown in Table S10. The docking results revealed that complexes **1**-**3** form stable complexes with DNA binding sites through non-covalent interactions [22]. The negative binding energies suggest that the complexes interact in a parallel manner with respect to the minor/major grooves of the DNA backbone. The resulting relative binding energies of **1**, **2**, and **3** with the DNA were obtained as -209.05 kJ/mol, -232.00 kJ/mol and -251.58 kJ/mol, respectively (Table S10). Thus complex

3, shows better binding affinity to the DNA molecule, while complex **1** displays the least affinity. The lower binding affinity of complex **1** may result from lack of planarity and its non-symmetrical nature, in good agreement with DFT studies. The relative binding energies of the investigated complexes were inversely proportional to the rates of ligand substitution reactions.

In summary, we have successfully synthesised and structurally characterised ruthenium(III) complexes of (pyrazolyl)pyridine ligands. The rate of ligand substitution reactions in the complexes is controlled by the electrophilicity of the metal centre. The mode of activation was found to be associative and the relative DNA binding affinities of the compounds are controlled by the structure of the complexes. The investigated compounds showed minimal cytotoxicity towards Hela cells. Investigations are underway both to expand the scope of the cancer cell lines used to assess compound cytotoxicity in addition to modification of the complex structures in order to improve the cell viability of the compounds.

Supplementary information

Supplementary materials contains the synthetic, kinetic, and biological assay procedures. Spectroscopic data for the compounds, related Figures for the kinetics plots, optimized geometries and biological studies are contained in supplementary materials.

Acknowledgements

The authors gratefully acknowledge financial support from the University of KwaZulu-Natal, National Research Foundation (NRF-South Africa) and Liverpool John Moores University. The authors wish to thank Meshack Sitati and Arumugam Jayamani for kinetic and molecular docking analyses, respectively.

References

[1] L. H. Kushi, C. Doyle, M. McCullough, C. L. Rock, W. Demark-Wahnefried, E. V. Bandera, S. Gapstur, A. V. Patel, K. Andrews, T. Gansler, American Cancer Society Guidelines on nutrition and physical activity for cancer prevention: reducing the risk of cancer with healthy food choices and physical activity". Ca. 62 (2012) 30–67.

[2] T. Karasawa, P. S. Steyger, An integrated view of cisplatin-induced nephrotoxicity and ototoxicity, Toxicol Lett. 237 (2015) 219-227.

[3] M. L. Krieger, N. Eckstein, V. Schneider, M. Koch, H. D. Royer, U. Jaehde, G. Bendas, Overcoming cisplatin resistance of ovarian cancer cells by targeted liposomes in vitro, Int. J. Pharm. 389 (2010) 10-17.

[4] T. Lazarević, A. Rilak, Ž. D. Bugarčić, Platinum, palladium, gold and ruthenium complexes as anticancer agents: Current clinical uses, cytotoxicity studies and future perspectives, Eur. J. Med. Chem. 142 (2017) 8-31.

[5] D. Lazić, A. Arsenijević, R. Puchta, Ž. D. Bugarčić, A. Rilak, DNA binding properties, histidine interaction and cytotoxicity studies of water soluble ruthenium(II) terpyridine complexes, Dalton Trans. 45 (2016) 4633-4646.

[6] A. Jayamani, M. Sethupathi, S. O. Ojwach, N. Sengottuvelan, Synthesis, characterization and biomolecular interactions of Cu(II) and Ni(II) complexes of acyclic Schiff base ligand, Inorg. Chem. Commun. 84 (2017) 144-149.

[7] P. Čanović, ; A. R. Simović, S. Radisavljević,I Bratsos, N. Demitri, M. Mitrović, Z. D. Bugarčić, Impact of aromaticity on anti-cancer activity of polypyridyl ruthenium(II) complexes: syntheses, structure, DN/protein binding, lipophilicity and anticancer activity, J. Biol. Inorg. Chem. 22 (2017) 1007-1028.

[8] I. Bratsos, E. Mitri, F. Ravalico, E. Zangrando, T. Gianferrara, A. Bergamo, E. Alessio, New half sandwich Ru(II) coordination compounds for anticancer activity, Dalton Trans. 41 (2012) 7358-7371.

[9] E. S. Antonarakis, A. Emadi, Ruthenium-based chemotherapeutics: are they ready for a prime time, Cancer Chemother. Pharmacol. 66 (2010) 1-9.

[10] W. X. Hong, F. Huang, T. Huan, X. Xu, Q. Han, G. Wang, H. Xu, S. Duan, Y. Duan, X. Long, Y. Liu, Z. Hu, Y. Liu, Comparative studies on DNA-binding and in vitro antitumor activity of enantiomeric ruthenium(II) complexes, J. Inorg. Biochem. 180 (2018) 54-60.

[11] G. S. Nyamato, M. Alam, S. O. Ojwach, M. P. Akerman, Nickel(II) complexes bearing (pyrazolyl)pyridines: synthesis, structures and ethylene oligomerization reactions, Appl. Organomet. Chem. 30 (2016) 89-94.

[12] A. O Ogweno, S. O. Ojwach, M. P. Akerman, (Pyridyl)benzoazole ruthenium(II) and ruthenium(III) complexes: role of heteroatom and ancillary phosphine ligand in the transfer hydrogenation of ketones Dalton Trans. 43 (2014) 1228-1237.

[13] W. Du, Q. Wang, L. Wang, Z. Yu, Ruthenium Complex Catalysts Supported by a Bis (trifluoromethyl) pyrazolyl–Pyridyl-Based NNN Ligand for Transfer Hydrogenation of Ketones, Organometallics, 33(2014) 974-982.

[14] M. T. Jackson, N. C. Duncan, B. Rich, M. E. Jones, K. A. Brien, M. Spiegel, C. M Garner, Synthesis, crystal structures, and characterization of the complexes of the bulky ligand 2, 6-bis-(3′, 5′-diphenylpyrazolyl) pyridine with ruthenium, rhodium, and palladium Polyhedron 139 (2018) 308-312.

[15] R. T. Edward, Structure, spectroscopic and angular-overlap studies of tris (pyrazol-1-yl) methane complexes, J. Chem. Soc. Dalton Trans. 4 (1993) 509-515.

[16] T. Astley, A. J. Canty, M. A. Hitchman, G. L. Rowbottom, B. W. Skelton, A. H. White, Structural, spectroscopic and angular-overlap studies of the nature of metal-ligand bonding for tripod ligands, J. Chem. Soc. Dalton Trans. 8 (1991) 1981-1990.

[17] J. O. Krause, O. Nuyken, K. Wurst, M. R. Buchmeiser, Synthesis and Reactivity of Homogeneous and Heterogeneous Ruthenium-Based Metathesis Catalysts Containing Electron-Withdrawing Ligands, Chem. Eur. J. 10 (2004) 777-784.

[18] D. P. Rillema, A. J. Cruz, C. Moore, K. Siam, A. Jehan, D. Base, T. Nguyen, W. Huang, Electronic and Photophysical Properties of Platinum (II) Biphenyl Complexes Containing 2, 2′-Bipyridine and 1, 10-Phenanthroline Ligands, Inorg. Chem. 52(2012) 596-607.

[19] H. Ertürk, A. Hofmann, R. Puchta, R. van Eldik, Influence of the bridging ligand on the substitution behaviour of dinuclear Pt(II) complexes. An experimental and theoretical approach, Dalton Trans. 22 (2007) 2295-2301.

[20] P. Čanović, A. R. Simović, S. Radisavljević, I. Bratsos, N. Demitri, M. Mitrović, Ž. D. Bugarčić, Impact of aromaticity on anticancer activity of polypyridyl ruthenium(II) complexes: synthesis, structure, DNA/protein binding, lipophilicity and anticancer activity, J. Biol. Inorg. Chem. 22(2017) 1007-1028.

[21] G. Matlashewski, L. Banks, D. Pim, L. Crawford, Analysis of human p53 proteins and mRNA levels in normal and transformed cells, Eur. J. Biochem. 154 (1986) 665–672.

[22] B. Tang, F. Shen, D. Wan, B.H. Guo, Y.J. Wang, Q.Y. Yia, Y.J. Liu, DNA-binding, molecular docking studies and biological activity studies of ruthenium(II) polypyridyl complexes, RSC Adv. 7(2017) 34945–34958.